Acta Cryst. (1997). B53, 18–24

Room-Temperature Structure and Geometrical Analysis of the Cubic–Tetragonal Phase Transition in Dodecasil 3C-THF

K. KNORR*† AND W. DEPMEIER

Mineralogisch-Petrographisches Institut der Christian Albrechts Universität zu Kiel, Olshausenstrasse 40, D-24098 Kiel, Germany. E-mail: knorr@hmi.de

(Received 13 June 1995; accepted 23 September 1996)

Abstract

The structure of dodecasil 3C-tetrahydrofuran $[Si_{68}O_{136}].4M$, $M = (CH_2)_4O$, at room temperature was determined from a merohedrally twinned crystal in the tetragonal space group $I4_1/a$. The deformation of the ideal framework at the cubic–tetragonal phase transition at $T_c \simeq 365$ K could be explained mainly by two different symmetry-breaking processes. (i) A tetragonal tetrahedron distortion of the Si(5) tetrahedra and (ii) a hitherto unknown local one-dimensional tilt mechanism, localized in the tetrahedral network. The location of the axes of this tilt system coincides with the positions of the fourfold inversion axes in the space group $I4_1/a$. At room temperature the tilt angle is $\varphi = 24°$. The symmetry properties of the tilt system can explain the reduction of space-group symmetry from the space group of the ideal structure $Fd\bar{3}m$ to the space group at ambient conditions $I4_1/a$. The guest molecule tetrahydrofuran does not fit the cage symmetry and has been found to be dynamically disordered. The average structure shows an off-center location in the $[5^{12}6^4]$ cage and follows the local $\bar{4}$ symmetry of the cage.

1. Introduction

Dodecasil-3C (D3C for short) belongs to the group of clathrasils (Liebau, 1985). It forms a SiO_4 tetrahedral framework. Its topology, first reported by Schlenker *et al.* (1981), can be described by two different types of cages. Fourfold face-connected pentagondodecahedra (cage symbol $[5^{12}]$) form pseudohexagonal nets which are stacked in an *abc* sequence. By this stacking a second type of cage, the hexacaidecahedra $[5^{12}6^4]$, is generated. In these cages various guest molecules can be accommodated. By analogy with the closest sphere packing, the *abc* stacking of the pseudohexagonal nets results in a structure of cubic symmetry, at least latent.

Depending upon the size and shape of the enclathrated molecules, different crystal metrics have been found at ambient conditions (Gies, 1984). A variety of reversible phase transitions is also known to exist from experimental methods, such as differential scanning calorimetry (DSC) or ^{29}Si MAS-NMR (Ripmeester, Desando, Handa & Tse, 1988; Tse, Desando, Ripmeester & Handa, 1993).

The highest possible symmetry is space group $Fd\bar{3}m$ with a lattice constant $a_0 \simeq 19.4$ Å. The space group $Fd\bar{3}m$ has been reported for spherical guest molecules (Kr, Xe, disordered CH_4) at room temperature, as well as for some high-temperature structures containing non-spherical molecules (Gies, 1984). For detemplated D3C the high-temperature space group is $Fd\bar{3}$ (Könnecke, Miehe & Fuess, 1992). Chae *et al.* (1991) reported a single-crystal structure refinement at room temperature in space group $I\bar{4}2d$ for D3C containing the guest molecule pyridine. X-ray Rietveld refinements of powder patterns are known in space group $I4_1/a$ for *tert*-butylamine and in space group *Fddd* for pyrrolidine as guest species (Könnecke, 1991).

In comparison to known silica polymorphs, extremely short Si—O distances (1.56–1.58 Å) and very large Si—O—Si angles (close to 180°) in connection with unlikely large thermal parameters for the framework oxygens are typical of the cited structure refinements. Disorder of the framework oxygens has been offered as an explanation for the deficiencies of the structure refinements. This fact points to the need for an exact measurement of the weak reflections, which carry the information on the host lattice disorder (Miehe, Vogt, Fuess & Müller, 1993).

Moreover, it has been found difficult to determine the positions of the guest molecules. Here, strong reflections at low Bragg angles are of special interest, because they carry the information about the orientation of the guest species. However, care must be taken when using Fourier methods since space-group symmetry ambiguities may lead to serious errors in the determination of template-atom positions in the case of pseudosymmetric frameworks (Hu & Depmeier, 1992).

2. Experimental

Crystals were grown hydrothermally in silica tubes with tetrahydrofuran (THF) as the template (Gies, Liebau & Gerke 1982). The crystals were examined by temperature-dependent high-resolution Guinier powder

† Present address: Hahn–Meitner Institut, NE, Glienicker Strasse 100, D–14109 Berlin, Germany.

set using *SHELXL*93 (Sheldrick, 1993). The program uses the method of Prett, Coyle & Ibers (1971) for the refinement of the twinned structure. The function minimized in the full-matrix least-squares procedure was $\Sigma w(F_o^2 - F_c^2)^2$. Scattering factors for neutral atoms were used (*International Tables for Crystallography*, Vol. C, 1992). The total number of variables of the framework refinement was 117, including one scale factor, one twin volume fraction parameter and 79 anisotropic thermal parameters of the 14 independent framework atoms. The weighting scheme proposed by the program $\{w = 1/[\sigma^2(F_o^2) + (aP)^2 + bP]$, with $P = \frac{1}{3}F_o^2(\max) - \frac{2}{3}F_c^2\}$ has been used. Under the assumption of a well defined framework stoichiometry, a refinement of population parameters of the framework atoms was considered unnecessary.

Anisotropic refinement of the framework atoms together with the twin component x converged at an intensity-based weighted R value, $wR_I = 0.13$ [conventional structure-factor-based R value $R_F = \Sigma(|F_o| - |F_c|)/\Sigma|F_o| = 0.045$]. Electron density in the $[5^{12}6^4]$ cage has been approximated by anisotropic refinement of the two strongest Difference Fourier (DF) maxima. In a final run with anisotropic simultaneous refinement of host- and guest-molecule atoms, a weighted intensity-based R value, $wR_I = 0.094$ (conventional $R_F = 0.034$), has been achieved for all 1176 reflections.

The reliability of the interpretation of the DF peaks as atomic positions has been tested by truncating the data set as proposed by Hu & Depmeier (1992). Difference maps have been calculated for two data sets with reduced resolution ($2\theta = 41°$, 961 reflections used; $2\theta_{max} = 35°$, 618 reflections used), as well as by omitting reflections with $I < a\sigma(I)$ ($a = 10$, 6, 3). For none of these trials could significant changes in the number of strongest DF peaks, their location or intensity be observed.

3. Results and discussion

The refined positional and equivalent thermal parameters are listed in Table 2. The volume fraction of the smaller twin component was found to be $x = 0.37$ (1). The tetrahedra connectivity is identical to that of the ideal symmetry of D3C. Fig. 1 shows the $[5^{12}]$ and $[5^{12}6^4]$ cages, respectively.

The anisotropic thermal parameters of Si revealed almost isotropic atomic displacement and gave no hint to any disorder. The number of independent Si positions is consistent with the findings of Tse, Desando, Ripmeester & Handa (1993), who reported five ^{29}Si MAS-NMR signals, the heights of which (1:4:4:4:4) agree with the multiplicity of the sites (4*a*) and (16*f*) in the space group $I4_1/a$. It should be noted, however, that despite this correspondence our space-group assignment is clearly distinct from the space group $I4_1/amd$, suggested by Tse, Desando, Ripmeester & Handa (1993). The Si atoms do not occupy the corresponding Wyckoff positions in either space group. For space group $I4_1/amd$ the positions are: (32*i*), (16*h*), (16*h*) and (4*a*).

The symmetry reduction pathway, starting from the aristotype and descending to the room-temperature structure of D3C-THF, is given in Fig. 2. It shows the standard cell choice with the body-centered cell for the

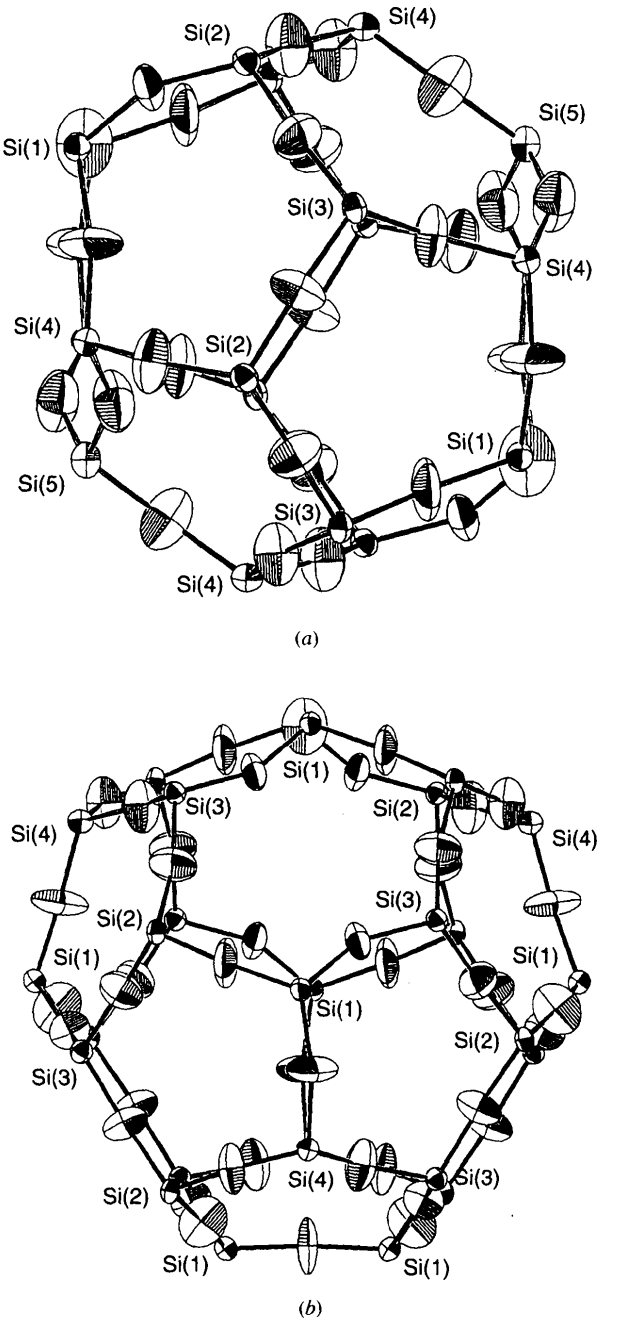

Fig. 1. *ORTEP* (Johnson 1965) drawing of the 50% thermal probability ellipsoids in the (*a*) pentagondodecahedra cage $[5^{12}]$ and (*b*) the hexacaidecahedra cage $[5^{12}6^4]$ in a (100) projection. For O atom labels refer to the connectivity table (Table 3*b*).

diffraction between 50 and 380 K, by thermal analysis (DSC, DTA and TG) and optical methods. At ambient conditions D3C-THF has been found to possess a body-centered tetragonal unit cell with $a_{tet} \simeq 2^{1/2}/2a_{cub}$ and $c_{tet} \simeq c_{cub}$. A reversible phase transition to the cubic phase happens at *ca* 365 K, detectable by a lattice parameter anomaly, as well as by DSC and hot-stage microscopy. Under crossed polarizers D3C-THF shows domains with domain walls parallel to pseudocubic {110} planes of the octahedrally shaped crystals. Such a pattern is typical for a ferroic phase transition. Details concerning the transition behavior will be discussed elsewhere.

For the data collection a 'pyramidally' shaped crystal fragment with a maximum edge length of *ca* 40 μm was selected. The same crystal was used for a preceding optical investigation using a polarizing microscope equipped with a spindle stage, which showed that the crystal consisted of a single domain. The uniaxial character of the optical indicatrix could also be confirmed.

2.1. *Data collection*

Mo $K\alpha$ radiation, graphite monochromator, MAR Research imaging plate system (180 mm detector diameter), distance crystal/detector 100 mm, exposure time 5 min per image, 69 images recorded, total number of reflections 12 138 ($2\theta_{max} = 44.9°$), Lorentz and polarization corrections, no absorption correction $\mu(\text{Mo } K_\alpha) = 0.71$ mm^{-1}, space group, determined from systematic absences, $I4_1/a$. In addition, the crystal was tested on a conventional four-circle STOE diffractometer performing Q scans along the pseudocubic and the tetragonal axes. Neither peak splitting nor superstructure reflections could be detected. All reflections exhibited sharp profiles with FWHM = 0.11° (full width at half-maximum). The data were processed using a modified version of the *MOSFLM* package (Leslie, Brick & Wonacott, 1986). Merging of all reflections according to Laue class 4/*m* with $R_I^2 = 0.039$ resulted in 1176 unique reflections [$R_I^2 = \Sigma(I - \langle I \rangle)^2/\Sigma I^2$]. All unique reflections, including very weak and negative reflections, were used in the refinement. Full experimental details are given in Table 1.*

2.2. *Structural model and refinement*

The structure refinement was started with a model which was transformed from the cubic phase (Könnecke, Miehe & Fuess, 1992) and refined by a distance least-squares procedure (Baerlocher, Hepp & Meier, 1977). Subsequent cycles of least-squares refinements (*SHELX*76; Sheldrick, 1976) in space group $I4_1/a$ allowed the reduction of R values to *ca* 0.22 without further improvement. Therefore, possible merohedral twinning has been taken into account. The space group $I4_1/a$ implies the possibility of merohedral twinning without the generation of additional reflections. Therefore, no higher-symmetric space group will be simulated by the twin law (*International Tables for Crystallography*, 1992, Vol. C). Twin elements are the {110} or {100} planes, which are symmetry elements of the holohedry (crystal class 4/*mmm*). The twinning operations transform the tetragonal axis a and b of the different twin individuals into each other. This superposition of the reciprocal lattices results in a mapping of the reflections (hkl) and $(khl)'$, with the primed indices referring to the second twin individual (Mazzi, Galli & Gottardi, 1976). In the refinement of the twinned structure one has to include only the volume fraction of the components as an additional refinable parameter for a refinement of the twinned data

Table 1. *Experimental details*

Crystal data	
Chemical formula	$17SiO_2.C_4H_8O$
Chemical formula weight	1113.6
Cell setting	Tetragonal
Space group	$I4_1/a$
a (Å)	13.684 (2)
c (Å)	19.482 (5)
V (Å^3)	3648 (2)
Z	4
D_x (Mg m^{-3})	1.991
Radiation type	Mo $K\alpha$
Wavelength (Å)	0.71069
μ (mm^{-1})	0.71
Temperature (K)	298
Crystal form	Pyramidal
Crystal size (mm)	0.040 × 0.040 × 0.028
Crystal color	Colorless
$F(000)$	2220
Data collection	
Diffractometer	MAR Research
Data collection method	Image plate
Absorption correction	None
No. of measured reflections	12 138
No. of independent reflections	1176
R_{int}	0.039
θ_{max} (°)	22.45
Range of h, k, l	$0 \rightarrow h \rightarrow 14$ $-9 \rightarrow k \rightarrow 10$ $0 \rightarrow l \rightarrow 20$
Refinement	
Refinement on	F^2
$R[F^2 > 2\sigma(F^2)]$	0.034
$wR(F^2)$	0.094
S	1.147
No. of reflections used in refinement	1176
No. of parameters used	117
H-atom treatment	H atoms not located
Weighting scheme	$w = 1/[\sigma^2(F_o^2) + (0.056P)^2 + 10.66P]$, where $P = 1/3[\max(F_o^2,0) + 2F_c^2]$
$(\Delta/\sigma)_{max}$	6.25
$\Delta\rho_{max}$ (e Å^{-3})	0.90
$\Delta\rho_{min}$ (e Å^{-3})	−0.31
Extinction method	None
Source of atomic scattering factors	*International Tables for Crystallography* (1992, Vol. C)

* Lists of anisotropic displacement parameters and structure factors have been deposited with the IUCr (Reference: SE0181). Copies may be obtained through The Managing Editor, International Union of Crystallography, 5 Abbey Square, Chester CH1 2HU, England.

Table 2. *Fractional atomic coordinates and equivalent isotropic displacement parameters (Å²)*

$$U_{eq} = (1/3)\sum_i \sum_j U^{ij} a_i^* a_j^* \mathbf{a}_i.\mathbf{a}_j.$$

	Wyckoff position	Site symmetry	x	y	z	U_{eq}
Si(1)	(16*f*)	1	−0.0086 (1)	0.1343 (1)	0.3709 (1)	0.012 (1)
Si(2)	(16*f*)	1	−0.3155 (1)	0.0693 (1)	0.0609 (1)	0.012 (1)
Si(3)	(16*f*)	1	0.7888 (1)	0.0569 (1)	0.4267 (1)	0.011 (1)
Si(4)	(16*f*)	1	−0.0010 (1)	0.4325 (1)	0.2169 (1)	0.012 (1)
Si(5)	(4*a*)	$\bar{4}$	0.0	1/4	0.1250	0.015 (1)
O(1)	(16*f*)	1	−0.3355 (3)	0.3226 (3)	−0.3316 (2)	0.029 (1)
O(2)	(16*f*)	1	0.8527 (3)	0.3637 (3)	0.8531 (2)	0.042 (1)
O(3)	(16*f*)	1	−0.6868 (3)	−0.0079 (3)	0.0081 (2)	0.042 (1)
O(4)	(16*f*)	1	−0.0068 (4)	0.4023 (4)	0.2944 (2)	0.052 (1)
O(5)	(16*f*)	1	0.1068 (3)	0.4660 (3)	0.1982 (2)	0.035 (1)
O(6)	(16*f*)	1	0.4246 (3)	0.5185 (3)	0.2980 (2)	0.038 (1)
O(7)	(8*e*)	2..	0.0	1/4	0.3738 (3)	0.043 (2)
O(8)	(16*f*)	1	0.2582 (3)	0.4878 (3)	0.1200 (2)	0.037 (1)
O(9)	(16*f*)	1	−0.0317 (3)	0.3411 (3)	0.1707 (2)	0.041 (1)
C	(16*f*)	1	0.521 (4)	0.677 (3)	0.145 (5)	0.032 (2)
O	(16*f*)	1	−0.448 (7)	0.258 (7)	−0.171 (4)	0.018 (3)

Table 3. *Selected geometric parameters (Å, °)*

Si(1)—O(2^{i})	1.583 (4)	Si(3)—O(3^{ix})	1.584 (4)
Si(1)—O(7)	1.5862 (13)	Si(3)—O(5^{vii})	1.598 (4)
Si(1)—O(4^{ii})	1.588 (4)	Si(4)—O(4)	1.567 (4)
Si(1)—O(1^{iii})	1.592 (4)	Si(4)—O(6^{x})	1.581 (4)
Si(2)—O(3^{iv})	1.587 (4)	Si(4)—O(5)	1.585 (4)
Si(2)—O(8^{ii})	1.597 (4)	Si(4)—O(9)	1.596 (4)
Si(2)—O(1^{v})	1.597 (4)	Si(5)—O(9^{ii})	1.592 (4)
Si(2)—O(6^{vi})	1.597 (4)	Si(5)—O(9^{xi})	1.592 (4)
Si(3)—O(8^{vii})	1.581 (4)	Si(5)—O(9^{xii})	1.592 (4)
Si(3)—O(2^{viii})	1.583 (4)	Si(5)—O(9)	1.592 (4)
O(2^{i})—Si(1)—O(7)	109.2 (2)	O(6^{x})—Si(4)—O(5)	109.9 (2)
O(2^{i})—Si(1)—O(4^{ii})	109.6 (3)	O(4)—Si(4)—O(9)	108.9 (3)
O(7)—Si(1)—O(4^{ii})	109.7 (3)	O(6^{x})—Si(4)—O(9)	108.0 (2)
O(2^{i})—Si(1)—O(1^{iii})	109.4 (2)	O(5)—Si(4)—O(9)	109.9 (2)
O(7)—Si(1)—O(1^{iii})	110.2 (2)	O(9)—Si(5)—O(9^{ii})	111.9 (4)
O(4^{ii})—Si(1)—O(1^{iii})	108.7 (3)	O(9)—Si(5)—O(9^{xi})	108.3 (2)
O(3^{iv})—Si(2)—O(8^{ii})	110.1 (2)	O(9)—Si(5)—O(9^{xii})	108.3 (2)
O(3^{iv})—Si(2)—O(1^{v})	107.9 (2)	O(9^{ii})—Si(5)—O(9^{xi})	108.3 (2)
O(8^{ii})—Si(2)—O(1^{v})	110.8 (2)	O(9^{ii})—Si(5)—O(9^{xii})	108.3 (2)
O(3^{iv})—Si(2)—O(6^{vi})	109.6 (2)	O(9^{xii})—Si(5)—O(9^{xi})	111.9 (4)
O(8^{ii})—Si(2)—O(6^{vi})	110.9 (2)	Si(1^{xiii})—O(1)—Si(2^{xiv})	150.8 (3)
O(1^{v})—Si(2)—O(6^{vi})	107.5 (2)	Si(1^{xv})—O(2)—Si(3^{xvi})	171.6 (3)
O(8^{vii})—Si(3)—O(2^{viii})	109.7 (3)	Si(3^{xvii})—O(3)—Si(2^{iv})	168.6 (3)
O(8^{vii})—Si(3)—O(3^{ix})	109.8 (2)	Si(4)—O(4)—Si(1^{ii})	168.9 (4)
O(2^{viii})—Si(3)—O(3^{ix})	109.7 (2)	Si(4)—O(5)—Si(3^{vi})	157.8 (3)
O(8^{vii})—Si(3)—O(5^{vii})	109.0 (2)	Si(4^{xviii})—O(6)—Si(2^{vii})	155.2 (3)
O(2^{viii})—Si(3)—O(5^{vii})	109.2 (2)	Si(1)—O(7)—Si(1^{ii})	175.9 (5)
O(3^{ix})—Si(3)—O(5^{vii})	109.4 (2)	Si(3^{vi})—O(8)—Si(2^{ii})	174.9 (3)
O(4)—Si(4)—O(6^{x})	109.9 (3)	Si(5)—O(9)—Si(4)	148.9 (3)
O(4)—Si(4)—O(5)	110.2 (3)		

Symmetry codes: (i) $\frac{1}{4}-y, x-\frac{3}{4}, \frac{5}{4}-z$; (ii) $-x, \frac{1}{2}-y, z$; (iii) $y-\frac{1}{4}, -\frac{1}{4}-x, \frac{3}{4}+z$; (iv) $-1-x, -y, -z$; (v) $y-\frac{3}{4}, -\frac{1}{4}-x, -\frac{1}{4}-z$; (vi) $\frac{1}{4}-y, x-\frac{1}{4}, z-\frac{1}{4}$; (vii) $\frac{1}{4}+y, \frac{1}{4}-x, \frac{1}{4}+z$; (viii) $\frac{5}{4}-y, x-\frac{3}{4}, \frac{5}{4}-z$; (ix) $\frac{3}{4}+x, y, \frac{1}{2}-z$; (x) $x-\frac{1}{4}, y, \frac{1}{2}-z$; (xi) $y-\frac{1}{4}, \frac{1}{4}-x, \frac{1}{4}-z$; (xii) $\frac{1}{4}-y, \frac{1}{4}+x, \frac{1}{4}-z$; (xiii) $-\frac{1}{4}-y, \frac{1}{4}+x, z-\frac{3}{4}$; (xiv) $-\frac{1}{4}-y, \frac{3}{4}+x, -\frac{1}{4}-z$; (xv) $\frac{3}{4}+y, \frac{1}{4}-x, \frac{5}{4}-z$; (xvi) $\frac{3}{4}+y, \frac{5}{4}-x, \frac{5}{4}-z$; (xvii) $x-\frac{1}{2}, y, \frac{1}{2}-z$; (xviii) $\frac{1}{2}+x, y, \frac{1}{2}-z$.

tetragonal space groups, containing half the number of atoms of the cubic F-centered cell. Nevertheless, the tetragonal space groups are *translationengleiche* subgroups of $Fd\bar{3}m$, because there is no change in the primitive cell of the space groups. The group–subgroup relations are given for the maximal *translationengleiche* subgroups (Bärnighausen 1980). It shows that the symmetry reduction from the cubic to the tetragonal crystal system corresponds to a transition to the lattice equivalent maximal subgroup of index 3. The second step of symmetry reduction involves the destruction of the tetragonal {110} and {100} mirror planes, resulting in space group $I4_1a$, which is again a *translationengleiche* subgroup, but now of index 2.

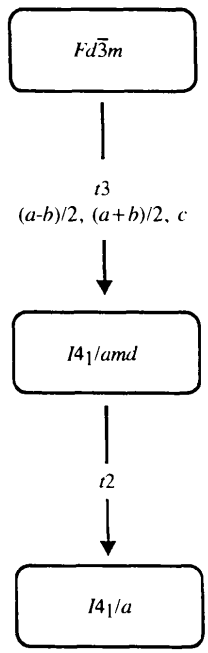

Fig. 2. Group–subgroup diagram of the symmetry reduction in D3C-THF in steps of maximum subgroups, using the conventional space-group setting.

Most important distances and angles within the clathrasil framework are given in Table 3. The distances d(Si—O) range between 1.567 (4) and 1.598 (4) Å, with an average of 1.588 (4) Å. The mean Si—O—Si angle is 163.6 (2)°. The minimum and maximum angles are 148.9 (3) and 175.9 (5)°, respectively. The equivalent thermal parameters U_{eq} of the framework oxygens are similar to those of other silica polymorphs. In contrast to the refinements of the cubic phases (Gies, 1984; Könnecke, Miehe & Fuess, 1992), no residual electron density has been found around the framework O atoms, which would have been indicative of local disorder. This is in agreement with the fact that our refined bond lengths are significantly longer than those of clathrasils with disordered framework O atoms (*ca* 1.56 Å).

Describing the structural changes of a tetrahedral framework one can distinguish between various symmetry-preserving or symmetry-breaking mechanisms (Depmeier, 1992). Here, the deformation of the tetrahedra and the question of the occurrence of a tilt system in this five-membered ring topology are of special interest.

The angular tetrahedron distortions of the SiO_4 tetrahedra with Si(1)–Si(4) as central atoms are rather small (Table 3*a*), with angles close to the ideal value (109.47°). The average bond lengths in these tetrahedra vary from 1.582 (4) to 1.594 (4) Å.

The Si(5) tetrahedron shows a perfectly tetragonal tetrahedron distortion (Depmeier, 1984) with a widening of two α angles of 2.4° and a narrowing of the remaining four angles such that the average O—Si—O angle is kept constant (*cf.* Fig. 3). This compression of the Si(5) tetrahedra results in a reduction of its volume by *ca* 0.2%. An important result of the tetrahedral distortion is the reduction of the local tetrahedra symmetry from $\bar{4}3m$ to $\bar{4}2m$ and, because of the special position of the Si(5) tetrahedra in $Fd\bar{3}m$, an ensuing change of the space-group symmetry from the ideal symmetry $Fd\bar{3}m$ to $I4_1/amd$.

A geometrical analysis of the pentagondodecahedra has been undertaken. We looked at the distortion of this cage by analyzing rotations and translations of the tetrahedra in comparison to the ideal structure. Following the procedure of Glazer (1972) we compared projections of the tetrahedra onto {100} planes of the unit cell with their cubic counterparts. We found a remarkable translation of *ca* 0.2 Å for the Si(2,3) tetrahedra and *ca* 0.1 Å for the Si(1) tetrahedra. For the tetrahedra Si(4,5) we found a pure rotation around axes, running parallel to **c** through the center of the tetrahedra, whereas for the Si(1–3) tetrahedra we have to state a complex motion of the tetrahedra, consisting of higher-dimensional rotations and translations. Corresponding to the notation of Glazer (1972), we denote the rotation of Si(4) by $a^0a^0c^-$ and for Si(5) by $a^0a^0c^+$. The rotation of the Si(4) tetrahedra is cooperative with respect to the counter-clockwise rotation of Si(5) and, therefore, termed tilt. Fig. 3 shows the location of a tilt axis running through a Si(5) tetrahedron, together with the tetragonal tetrahedra distortion of this type of tetrahedra. Since this one-dimensional rotation is not extended to the remaining tetrahedra, we term the tilt system local. The rotational axes of the Si(5) tetrahedra coincide with all $\bar{4}$ axes of the space group $I4_1/a$. The cooperative action of the tilt system and the definition of the tilt angle is shown in Fig. 4.

There are two O(9)—O(9′) tetrahedron edges of the Si(5) tetrahedra in the ideal structure, which are parallel to the *a* and *b* axes of the tetragonal unit cell or < 110 > of the cubic cell, respectively. The distortion of the ideal structure to the room-temperature structure results in a counter-clockwise tilting of the Si(5) tetrahedra, such that the tilt angle φ is enclosed between the tetragonal *a* or *b* axes and the O(9)—O(9′) tetrahedron edge. At room temperature the tilt angle is large with a value of $\varphi = 24°$. Normally a volume decrease has to be noted for structures with an active tilt system and, in fact, temperature-dependent powder diffraction shows a volume decrease of *ca* 0.7% (Knorr & Depmeier, 1993).

In contrast to the tetrahedron distortion, the tilt preserves the local tetrahedral symmetry. Regardless of whether one starts in $Fd\bar{3}m$ or $I4_1/amd$ as a high-symmetry phase, the transition governed by the tilt of the Si(5) tetrahedra is connected with the removal of the cubic (..*m*) or the tetragonal (.*m*.) mirror planes. Thus, the space group $I4_1/a$ is the highest possible symmetry compatible with the described tilt system.

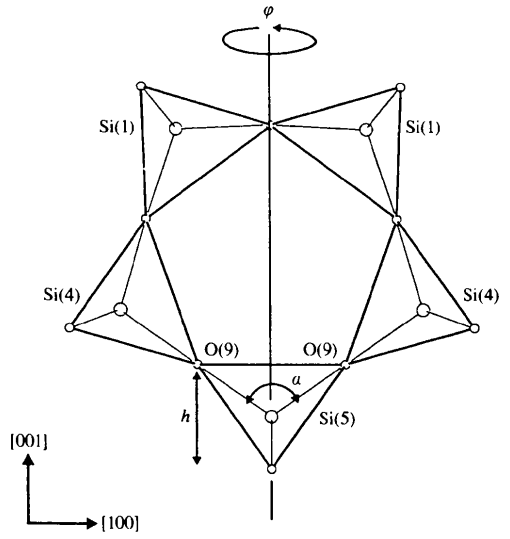

Fig. 3. Projection of a five-membered ring parallel (010) to the $[5^{12}]$ cage using *CELLGRAF* (Reck, Kretschmer & Walther, 1992), showing the tetragonal tetrahedra deformation of a Si(5) tetrahedron (angle α) and the location of a $\bar{4}$ tilt axis with tilt angle φ.

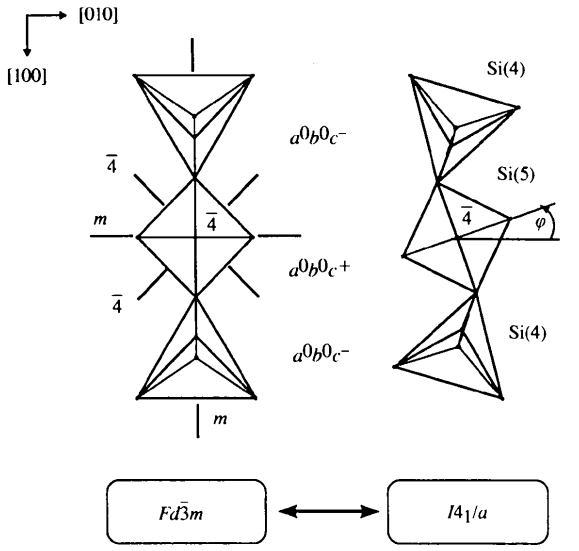

Fig. 4. Tetrahedra drawing (Reck, Kretschmer & Walther, 1992) in a (001) projection presenting the definition of the tilt angle φ and the counter-clockwise rotation of the Si(5) tetrahedron with respect to the tetragonal cell.

Discussing the orientation of the THF molecule in the $[5^{12}6^4]$ cage, one has to be aware of the symmetry-breaking geometry of the molecule. Neither the twofold symmetry of the envelope conformation nor the asymmetric twisted envelope conformation of the THF molecule matches the $(\bar{4})$ site symmetry of the center of the $[5^{12}6^4]$ cages. Thus, in space group $I4_1/a$ one has to assume a dynamically or statically disordered THF molecule. From thermal analysis it is known that there is one THF molecule per $[5^{12}6^4]$ cage. As pointed out in the *Experimental*, we found two maxima of intensity at 1.31 and 1.25 e Å^{-3}, respectively. Several additional DF peaks of lower intensity could also be found in this cage. An arbitrary assignment of an O atom and a C atom to the strongest and the second strongest DF peak, respectively, and anisotropic refinement of this model produced a cluster of atoms which might be interpreted as superimposed THF molecules, as shown in the inset of Fig. 5. However, we have to note that in this simplified model C and O atoms in the cluster are partly symmetry related by $\bar{4}$. A refinement with restrained bond lengths of a THF molecule built from five independent atoms did not improve the result.

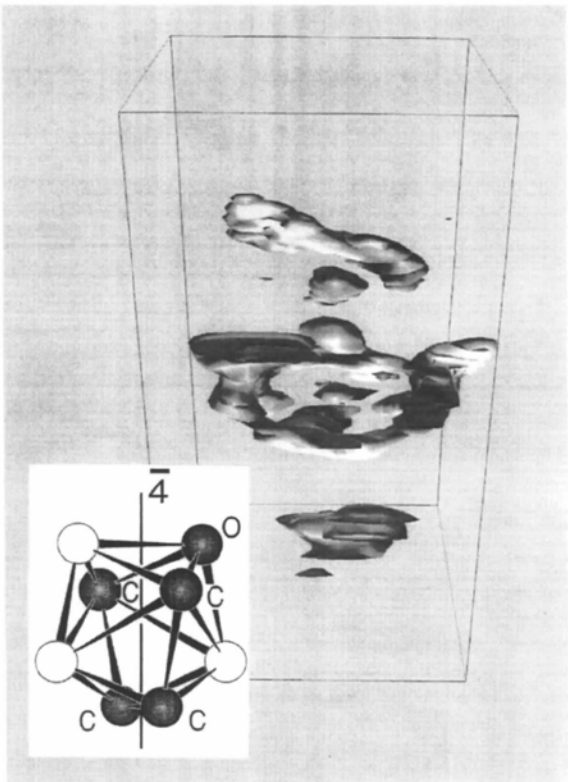

Fig. 5. Electron-density isosurfaces (Advanced Visual Systems Inc., 1992) of ~0.5 e Å^{-3} in the $[5^{12}6^4]$ cage, calculated by Fourier reconstruction with *SHELX*76 (Sheldrick 1976). View parallel to [010]. The inset shows a simplified ball-and-stick model of disordered THF molecules (Nolze & Kraus, 1994). One possible orientation is highlighted; H atoms are omitted.

In comparison to bond lengths given by *International Tables for Crystallography* (1992, Vol. C), the average C—O [1.34 (7) Å] and C—C distances [1.37 (7) Å] in the cluster are significantly too short. This and the unrealistically high temperature factors are commonly accepted as the expression of the strong orientational disorder. Fig. 5 shows a Fourier reconstruction of the electron density in the $[5^{12}6^4]$ cage. Plotted are isosurfaces of ~0.5 e Å^{-3}. It clearly shows that the density distribution is broad and poorly localized. This and the recently, by means of quasielastic neutron scattering, found fast reorientation motion with a correlation time, $\tau \simeq 0.2$ ps (Knorr, Krimmel & Güthoff, 1996), are indicative of dynamical disorder of the molecule in the cage. Therefore, orientation as well as the conformation of the THF molecule are not unambiguous.

We refrain from an attempt to interpret the residual electron density in the cage further in terms of a static superposition of several molecules. Without further information we prefer to believe that our observations reflect deficiencies of the model and unavoidable experimental uncertainties of the measurement.

A refinement of the residual electron density of 0.9 e Å^{-3} at the center of the $[5^{12}]$ cage has no significant influence on the structural model. The density might be attributed to impurities during crystal growth or artefacts of the refinement due to the pseudosymmetric nature of the described system.

The authors would like to thank Professor H. Gies for supplying the crystals of D3C, Dr Ch. Betzel for recording the data set on the imaging plate at the EMBL Hamburg and Dr F. Mädler (HMI Berlin) for technical assistance with AVS. Financial support of this work by the Deutsche Forschungsgemeinschaft under contract DE 412/5-1,2 is gratefully acknowledged.

References

Advanced Visual Systems Inc. (1992). Waltham, Massachusetts, USA.

Baerlocher, C., Hepp, A. & Meier, W. (1977). *DLS*76. *A Program for the Simulation of Crystal Structures by Geometric Refinement*. Zürich, Switzerland: ETH.

Bärnighausen, H. (1980). *MATCH Commun. Math. Chem.* **9**, 139–175.

Chae, H. K., Klemperer, W. G., Payne, D. A., Suchicital, C. T. A., Wake, D. R. & Wilson, S. R. (1991). *New Materials for Nonlinear Optics*. ACS Symposium Series.

Depmeier, W. (1984). *Acta Cryst.* B**40**, 185–191.

Depmeier, W. (1992). *Z. Kristallogr.* **199**, 75–89.

Gies, H. (1984). *Z. Kristallogr.* **167**, 73–82.

Gies, H., Liebau, F. & Gerke, H. (1982). *Angew. Chem.* **94**, 214–215.

Glazer, A. M. (1972). *Acta Cryst.* B**28**, 3384.

Hu, X. & Depmeier, W. (1992). *Z. Kristallogr.* **201**, 99–111.

Johnson, C. K. (1965). *ORTEP*. Report ORNL-3794. Oak Ridge National Laboratory, Tennessee, USA.

Knorr, K. & Depmeier, W. (1993). *Z. Kristallogr.* Suppl. 7, 31.
Knorr, K., Krimmel, A. & Güthoff, F. (1996). *Quasielastic Scattering of D3C-THF, BeNSC Experimental Reports.* In the press.
Könnecke, M. (1991). Ph.D. Thesis. TU, Darmstadt.
Könnecke, M., Miehe, G. & Fuess, H. (1992). *Z. Kristallogr.* **201**, 147–155.
Leslie, A. G., Brick, P. & Wonacott, A. J. (1986). *CCP4 Newsl.* **18**, 233–239.
Liebau, F. (1985). *Structural Chemistry of Silicates: Structure, Bonding and Classification.* Berlin, Heidelberg: Springer Verlag.
Mazzi, F., Galli, E. & Gottardi, G. (1976). *Am. Mineral.* **61**, 108–115.
Miehe, G., Vogt, T., Fuess, H. & Müller, U. (1993). *Acta Cryst.* B**49**, 745–754.
Nolze, G. & Kraus, W. (1994). *PowderCell* 1.5. BAM, Berlin.
Prett, C. S., Coyle, B. A. & Ibers, J. A. (1971). *J. Chem. Soc.* pp. 2146–2151.
Reck, G., Kretschmer, R. G. & Walther, G. (1992). *CELLGRAF. Program for Representation of Organic and Inorganic Crystal Structures.* Bundesanstalt für Materialforschung.
Ripmeester, J. A., Desando, M., Handa, Y. P. & Tse, J. S. (1988). *J. Chem. Soc. Chem. Commun.* pp. 608–611.
Schlenker, J. L., Dwyer, F. G., Jenkins, E. E., Rohrbaugh, W. J., Kokotailo, G. T. & Meier, W. M. (1981). *Nature*, **294**, 340–341.
Sheldrick, G. M. (1976). *SHELX*76. *Program for Crystal Structure Determination.* University of Cambridge, England.
Sheldrick, G. M. (1993). *SHELXL*93. *Program for Crystal Structure Refinement.* University of Göttingen, Germany.
Tse, J. S., Desando, M., Ripmeester, J. A. & Handa, Y. P. (1993). *J. Am. Chem. Soc.* **115**, 281–284.